Received: 7 October 2020 | Revised: 6 January 2021 | Accepted: 18 January 2021

DOI: 10.1111/ppa.13353

ORIGINAL ARTICLE

Plant Pathology | WILEY

Pewenomyces kutranfy gen. nov. et sp. nov. causal agent of an important canker disease on *Araucaria araucana* in Chile

Felipe Balocchi[1] | Mike J. Wingfield[2] | Rodrigo Ahumada[3] | Irene Barnes[2]

[1]Department of Plant and Soil Science, FABI, University of Pretoria, Pretoria, South Africa

[2]Department of Biochemistry, Genetics and Microbiology, Forestry and Agricultural Biotechnology Institute (FABI), University of Pretoria, Pretoria, South Africa

[3]Bioforest S.A., Concepcion, Chile

Correspondence
Irene Barnes, Department of Biochemistry, Genetics and Microbiology, FABI, University of Pretoria, Pretoria, 0002, South Africa.
Email: irene.barnes@fabi.up.ac.za

Abstract

Araucaria araucana, (commonly referred to as araucaria, pewen, or monkey puzzle tree) is an ancient conifer endemic to the Chilean and Argentinian mountain ranges where it has a sacred relevance to indigenous communities. During 2015, a serious disease was noticed on trees of all ages in most of the natural distribution of this iconic tree. Four areas were surveyed, and the most important symptoms of the disease were cankers on branches and stems resulting in copious resin exudation. Trees were monitored for a period of two years and isolations were made from the cankers. Field observations showed that the disease typically begins on the leaves or at the leaf bases and progresses downwards to initiate cankers that can girdle branches or stems within a two-year period. Black ascomata, resembling those of *Caliciopsis* species previously described from *A. araucana*, were consistently found developing in the cankers from which isolations were made. Phylogenetic analyses of the ITS, nucSSU, and nucLSU gene regions showed that the fungus resides in the Coryneliaceae but is distinct from other genera in that family. The morphological characteristics and phylogenetic position of the fungus show that it represents a new genus and species, described here as *Pewenomyces kutranfy* gen. nov. et sp. nov. Pathogenicity trials on trees under field conditions confirmed that this newly described fungus is able to cause cankers on *A. araucana* similar to those found under natural conditions.

KEYWORDS

canker pathogen, Coryneliaceae, disease emergence, novel genus, novel taxon, pewen

1 | INTRODUCTION

Araucaria araucana (araucaria, pewen, or pehuén) is an ancient conifer endemic to the Chilean and Argentinian mountain ranges, distributed from ~37°24′ to ~40°03′ S. It is a dioecious, evergreen tree, with an extended lifespan and is adapted to grow at high altitudes and low temperatures, including at least three months of snow (González & Veblen, 2006). The tree is sacred to the Mapuche people who represent one of the largest indigenous cultures in Chile (Herrmann, 2005; Rodriguez et al., 1983). The genus *Araucaria* resides in the Araucariaceae, along with the genera *Agathis* and *Wollemia*, both of which are mostly distributed in the southern Asia–Pacific region. *A. araucana* and *Araucaria angustifolia* (Brazilian pine) are the only two extant species in the genus and family that are native to South America (Kershaw & Wagstaff, 2001).

During 2015, severe crown disease symptoms were observed on *A. araucana* trees in most of its natural range in Chile (CONAF, 2018) and Argentina (Vélez et al., 2020). Trees exhibited a variety of symptoms on their leaves and branches, leading to the hypothesis that the problem could be related to abiotic factors and stress, potentially including climate change. Furthermore, it was suggested that such stress could predispose the trees to damage by native pests and pathogens (Vélez et al., 2018).

Very little is known regarding the diseases of *A. araucana* in its natural environment. Several pathogens have been recorded, including the heteroecious rust *Mikronegeria fagi*, some minor leaf pathogens such

as *Rhizothyrium parasiticum* and *Phaeocryptopus araucariae*, and root rot caused by *Armillaria mellea* sensu lato (Butin, 1970, 1975, 1986; Butin & Peredo, 1986; González & Opazo, 2002). The identification of all the fungi associated with these diseases was based only on morphology and came at a time when there was no DNA sequence-based phylogenetic inference able to confirm their taxonomic placement. Additionally, most of these pathogens have been referred to only once in the literature, illustrating the scarcity of the information available on them.

More recent studies on *A. araucana* have led to the description of several fungi on these trees, although little is known regarding their role in causing disease. These include *Diplodia africana*, *Diplodia mutila*, and *Neofusicoccum nonquaesitum* residing in the Botryosphaeriaceae, and two species of *Mortierella* (Mortierellales: Mortierellomycotina), namely *Mortierella alpina* and *Mortierella* sp. (Vélez et al., 2020). *D. africana* was associated with twig die-back on a single *A. araucana* tree within its natural distribution (Zapata & Schafer, 2019), and *D. mutila* and *N. nonquaesitum* were found on ornamental trees outside their natural range (Besoain et al., 2017; Pérez et al., 2018). The two *Mortierella* species were seldom recovered, and each was only recorded from a single location in the Argentinian *Araucaria* population (Vélez et al., 2020). None of these fungi are known to be primary pathogens and they appear to be associated with localized problems rather than linked to a widely distributed disease.

A preliminary inspection of diseased *A. araucana* trees conducted in 2017 by M. J. Wingfield and R. Ahumada (unpublished data) revealed that affected trees consistently had severe cankers on their branches and stems. This led to more intensive surveys where a fungus resembling a *Caliciopsis* sp. (Coryneliaceae) was consistently found sporulating on mature cankers. Two species of *Caliciopsis*, *Caliciopsis brevipes* and *Caliciopsis cochlearis*, have been morphologically described from *A. araucana* in Chile (Butin, 1970). One of these, *C. brevipes*, was associated with leaf deformation (Butin, 1970) but no pathogenicity tests have been conducted with the fungus. The other species, *C. cochlearis*, is known as a saprophyte on dying leaves and decaying bark of several conifers including *A. araucana* (Butin, 1970, 1986).

The objectives of this study were to conduct surveys of the canker disease on *A. araucana* in Chile and to monitor the progression of the disease symptoms over time. In addition, isolations were made from cankers, and specifically of the fungus resembling a species of *Caliciopsis* consistently associated with this symptom, for identification purposes. The fungus was identified based on multigene phylogenetic inferences using DNA sequence data from the nucLSU, nucSSU, and ITS gene regions, as well as morphological characteristics. Its pathogenicity was also considered in inoculation tests.

2 | MATERIALS AND METHODS

2.1 | Monitoring of disease symptoms

Several field surveys were conducted of Chilean National Parks and private land-holdings where *A. araucana* forests occur. These included Ralco National Reserve, Conguillío National Park, and Villarrica National Park in the Andes mountain range and private properties in Trongol Alto in the coastal range (Nahuelbuta; Figure 1). These surveys focused on monitoring stem and branch cankers to determine their distribution and disease progress over time. Trees with cankers at different stages of development were monitored at four time points between December 2017 and December 2019. A total of 27 trees at different locations were selected and marked, and branches on these trees were labelled. All the trees were GPS referenced, and photographic images were captured for them in December 2017, April 2018, February 2019, and December 2019. This made it possible to track the progression of disease symptoms from the first appearance of small sites of discolouration to the eventual death of the branches.

2.2 | Collection of samples and isolation of fungi

Branch canker samples were collected during December 2017 and January 2018 from the survey sites described above (Figure 1). Five collection points were established at each site except for Trongol Alto, which had three collection sites. Five samples from different trees were collected at each sampling point. Samples consisted of 20–60 cm branch segments bearing fresh, resinous cankers. Seven stem cankers were also collected at later stages from Conguillío National Park, three during December 2018, and four during December 2019.

For fungal isolations, all healthy leaves surrounding the cankers were removed and affected leaves were cut to their bases to reveal the discoloured tissue. This material was then briefly surface-disinfested by immersion in 70% ethanol for 10 s and 5% sodium hypochlorite for 1 min, and then rinsed with sterile distilled water. Outer layers of discoloured tissue were removed and small pieces of tissue were dissected from the margins of the discoloured area and plated on Petri dishes containing 50% potato dextrose agar (19.5 g/L PDA, 10 g/L agar; Merck) or 2% malt extract agar (MEA, 20 g/L malt extract, 20 g/L agar; Biolab). Isolations were incubated at 20–25 °C for 14 days and the obtained fungi were transferred to fresh 2% MEA plates. All isolates were then transferred to 2% water-agar (WA, agar 20 g/L; Biolab) and grown for 2–4 days, after which single hyphal tips were isolated and transferred to 2% MEA on Petri dishes.

In addition to isolations from diseased tissues, single spore isolations were made directly from fruiting bodies (ascomata) present in cankers on branches. In these cases, whole fruiting bodies were each placed on the surface of WA in Petri dishes and rolled across the agar surface using a sterile dissecting needle to release the spores. After 24–48 hr incubation, germinating spores were individually transferred to new Petri dishes containing 2% MEA. Isolates were broadly grouped into morphotypes based on colony shape and colour.

2.3 | DNA extraction, PCR, and sequencing reactions

Isolates representing a dominant fungal morphotype obtained from isolations from lesion margins and fruiting bodies were selected for

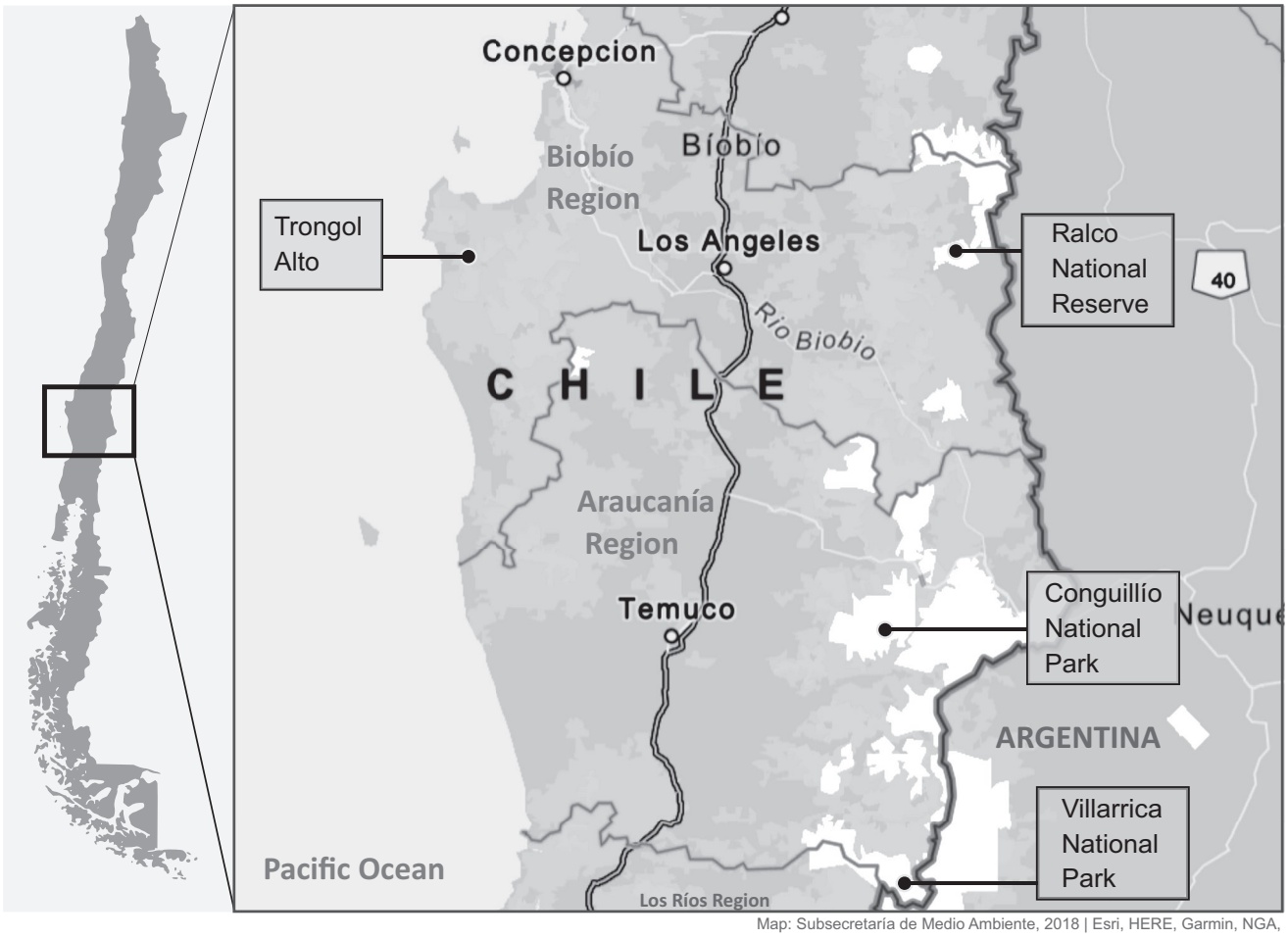

Site / Collection point	Ralco National Reserve	Conguillío National Park: Los Paraguas	Villarrica National Park: Puesco	Trongol Alto
Point 1	-37.964705° , -71.327459°	-38.697836° , -71.817216°	-39.570510° , -71.502642°	-37.553434° , -73.188438°
Point 2	-37.962620° , -71.327679°	-38.698653° , -71.816826°	-39.572706° , -71.499235°	-37.571061° , -73.194365°
Point 3	-37.954698° , -71.331507°	-38.697493° , -71.814460°	-39.575582° , -71.493489°	-37.564893° , -73.205764°
Point 4	-37.951548° , -71.333419°	-38.698075° , -71.813826°	-39.581883° , -71.478997°	- -
Point 5	-37.949798° , -71.337132°	-38.697527° , -71.815577°	-39.584783° , -71.470167°	- -

FIGURE 1 Location of the study sites within the natural range of *Araucaria araucana* in the Andes mountain range and Coastal range. GPS coordinates for each sampling point within each site are provided

sequence comparison. Pure cultures of these isolates were grown on 2% MEA for 7–21 days for DNA extractions. Mycelium was collected and placed in 2 ml Eppendorf tubes, freeze-dried overnight and then ground in 2 ml Eppendorf tubes with metal beads using a mixer mill (MM 301, Retsch GmbH) set at 30 oscillations/s for 3 min. A phenol/chloroform protocol, described in Barnes et al. (2001) was used to extract DNA, with the exception of the first centrifuge stage being carried out for 60 min at 4 °C rather than at room temperature. RNase was added after the final suspension and incubated at 65 °C for 60 min. DNA concentrations were measured with a NanoDrop spectrophotometer (Thermo Scientific NanoDrop ND-1000) and standardized to 30 ng/µl working stock for PCRs.

The internal transcribed spacer (ITS) gene region was amplified with the primers ITS1/ITS4 (White et al., 1990) for all the isolates, and a subsequent group of isolates was selected to amplify the large ribosomal subunit (nucLSU) using the primers LROR/LR5 (Rehner & Samuels, 1995; Vilgalys & Hester, 1990) and the small ribosomal subunit (nucSSU) with the primers NS1/NS3/NS4/NS8 (White et al., 1990). PCRs were carried out using MyTaq DNA polymerase (Bioline) in 25 µl reactions containing 5 µl of MyTaq Reaction Buffer 5×, 0.5 µl of 10 µM of each primer, 0.3 µl DNA polymerase, and 17.7 µl of sterile distilled water (SABAX). The thermal cycling conditions included an initial denaturation stage of 95 °C for 3 min; followed by 35 cycles of denaturing at 95 °C for 30 s, annealing at 56 °C for 30 s and elongation at 72 °C for 45 s; and a final elongation stage at 72 °C for 4 min. PCR amplicons were stained with GelRed (2 µl per 4 µl of PCR product) and electrophoresis was carried out by running the product on a 1% agarose gel for 12 min at 110 V.

PCR amplicons were cleaned by sodium acetate precipitation (Duong et al., 2013) and eluted in sterile distilled water. The forward and reverse sequences were separately sequenced using the BigDye Terminator Cycle Sequencing Ready Reaction Kit (Applied Biosystems, Thermo Fisher) following the manufacturer's protocol. The obtained products were cleaned using sodium acetate precipitation. Sequencing of the products was carried out at the Bioinformatics and Computational Biology Unit, University of Pretoria. The forward and reverse sequences obtained for each isolate were visualized and assembled into consensus sequences with CLC Main Workbench v. 8.0.1 (https://digitalinsights.qiagen.com/products-overview/discovery-insights-portfolio/analysis-and-visualization/qiagen-clc-main-workbench/).

2.4 | Phylogenetic analyses

Consensus sequences were aligned to NCBI's GenBank database (NCBI, http://www.ncbi.nlm.nih.gov) using the BLAST utility to obtain a preliminary identification of all isolates. Based on the similarity output results, sequence data sets were generated for the ITS, nucLSU, and nucSSU gene regions available in GenBank for taxa relevant in determining the phylogenetic placement of the fungus (Table 1). This included isolates of most sequenced species residing in the Coryneliaceae, representative species for all subclasses in the Eurotiomycetes, and three species of Lecanoromycetes that served as the outgroup. Selection of isolates was made favouring ex-type cultures and/or cultures that had most of the gene regions sequenced. Additional sequences were produced, following the same methods described above, for two isolates (CBS 140.64 and CBS 142066) obtained from the culture collection of the Westerdijk Fungal Biodiversity Institute, Utrecht, Netherlands (CBS) and these were included in the sequence data sets.

The sequences in the databases were aligned using the online version of MAFFT (Katoh et al., 2019) (https://mafft.cbrc.jp/alignment/server/), and visualized and edited with MEGA v. 7.0.26 (Kumar et al., 2016). The sequences for each gene region were first aligned separately for individual phylogenetic analyses and then concatenated using CLC Bio Main Workbench to perform a combined analysis of the three gene regions. Maximum-likelihood trees for the four data sets (the individual sequences and the concatenated sequence) were generated with IQ-Tree Web server (Trifinopoulos et al., 2016) (http://iqtree.cibiv.univie.ac.at/) using the model ranked best according to the Bayesian information criterion (BIC) by ModelFinder (Kalyaanamoorthy et al., 2017). Bayesian inference trees for all four data sets were performed with Mr Bayes v. 3.2.6 by the Markov chain Monte Carlo (MCMC) method with four independent chains. Ten million generations with sampling every 100 steps were performed. Stationarity was corroborated by visualizing the data with Tracer v. 1.6.0 and burn-in was set to the first 10% of generations. Phylogenetic trees were visualized and edited with FigTree v. 1.3.1, iTOL v. 4 (https://itol.embl.de/), and Inkscape v. 0.92.4.

2.5 | Morphology

Ascomata and spermogonia were collected from plant material and cultures photographed and measured using a Zeiss SteREO Discovery.V.12 modular stereomicroscope and the software AxioVision (AxioVs40x64 v. 4.9.1.0). A total of 14 ascomata and five spermogonia were measured from canker samples, and 10 additional spermogonia were measured from 3-month-old cultures on MEA. Ascomata and spermogonia were also used to prepare semipermanent slides in lactic acid sealed with nail polish. Ascomata were cut with a microtome (Leica CM1520). Measurements of 19 asci, 50 ascospores, and 25 spermatia from cankers and 50 spermatia from cultures were made using the Nikon Eclipse Ni-u microscope with a Nikon DS-Ri2 camera and the software NIS-Elements v. 4.30.

Four representative isolates (CMW54230, CMW54240, CMW54244, and CMW54251) obtained from different trees and from three different sites were selected to study culture growth and characteristics. For this purpose, cultures were grown at temperatures ranging from 5 to 35 °C in 5 °C intervals on 2% MEA and oatmeal agar (OMA) in 90 mm Petri dishes in the dark. The area of culture growth was traced on the plates with a marker pen every 4 days for 28 days with three replicates of each isolate at each temperature. The total area of the cultures was measured using image processing with ImageJ software (Guerrero et al., 2012; Wang, 2017). In the case of cultures at temperatures where there was no growth, these were incubated for an additional 14 days at 20 °C to assess the viability of the original inoculum. Colours of cultures were designated according to the colour charts of Rayner (1970).

2.6 | Pathogenicity tests

Two isolates obtained from cankers (CMW54240 and CMW54244) were used for pathogenicity tests conducted on *A. araucana* trees during December 2018 in Villarrica National Park sector Puesco, where they had originally been collected. Isolates were grown on PDA at 20 °C for 14 days prior to inoculation. Trees chosen for inoculation were randomly distributed in two areas of approximately 1 ha, in open areas and under canopy cover. Healthy branches of trees between 1.5 and 3 m in height were inoculated by removing a leaf segment and placing a plug of mycelium-colonized agar onto the wounds, which was subsequently covered with Parafilm to avoid contamination and desiccation. A single branch was inoculated on each of six trees for each of the isolates and the control (sterile PDA plugs).

After 6 weeks, inoculated branch segments were cut from the trees and transferred in brown paper bags to the laboratory for assessment. Leaves were removed from the branches, the bark removed with a sterile scalpel to expose discolouration, and lesion lengths (mm) were measured. The percentage of the branch that had been girdled was measured by cutting the lesions transversely at the point of inoculation, capturing an image of the section, and

TABLE 1 Details of cultures and gene regions used for phylogenetic analyses

Taxonomic position	Species	Isolate	GenBank accession no.		
			ITS	nucLSU	nucSSU
Eurotiomycetes					
Chaetothyriomycetidae					
Chaetothyriales					
Cyphellophoraceae	*Cyphellophora guyanensis*	MUCL 43737 ET	NR132880.1	KC455253.1	NG065005.1
	Cyphellophora laciniata	CBS 190.61 ET	JQ766423.1	FJ358239.1	FJ358307.1
Pyrenulales					
Pyrenulaceae	*Pyrenula nitida*	F-5929	JQ927458.1	DQ329023.1	–
	Pyrgillus javanicus	AFTOL-ID 342	DQ826741.1	DQ823103.1	DQ823110.1
Verrucariales					
Verrucariaceae	*Verrucaria lecideoides*	AFTOL-ID 2295	EU010256.1	EF643798.1	–
	Verrucaria muralis	AFTOL-ID 2265	EU010261.1	EF643803.1	EF689878.1
Coryneliomycetidae					
Coryneliales					
Coryneliaceae	*Caliciopsis beckhausii*	MA 18186 NT	NR132090.1	NG060418.1	–
	Caliciopsis calicioides	Voucher 211	JX968549.1	–	–
	Caliciopsis eucalypti	CBS 142066 ET	NR154836.1	NG059013.1	**MT359910**
	Caliciopsis indica	GFCC 4947 ET	NR119752.1	GQ259980.1	–
	Caliciopsis orientalis	AFTOL-ID 1911/CBS 138.64 ET	NR145392.1	NG058741.1	DQ471039.1
	Caliciopsis pinea	AFTOL-ID 1869/CBS 139.64	KP881691.1	DQ678097.1	DQ678043.1
	Caliciopsis pseudotsugae	CBS 140.64 ET	**MT334517**	**MT334518**	**MT359911**
	Caliciopsis valentina	MA 18176/IGB290 T	NR132091.1	NG060419.1	–
	Corynelia africana	PREM 57242/ARW 247 T	NR153901.1	NG058910.1	KP881719.1
	Corynelia fructigena	PREM 57240/ARW 250 T	NR153902.1	NG058911.1	KP881720.1
	Pewenomyces kutranfy	CMW54230 PT	**MT334514**	**MT334519**	**MT359912**
	P. kutranfy	CMW54240 ET	**MT334515**	**MT334521**	**MT359913**
	P. kutranfy	CMW54244 PT	**MT334516**	**MT334520**	**MT359914**
	Hypsotheca eucalyptorum	CBS 145576 T	MK876393.1	MK876434.1	–
	Hypsotheca maxima	CPC 24674/COAD 1983 eT	NR160329.1	NG064416.1	–
	Hypsotheca nigra	MA 18191/ IGB305	–	KP144011.1	–
	Hypsotheca pleomorpha	CPC 32144/CBS 144636	MK442588.1	MK442528.1	–
	Lagenulopsis bispora	PREM 57232/ARW 249 eT	NR154120.1	NG060325.1	NG061200.1
	Tripospora tripos	PREM 61200/ARW 677	KP881712.1	KP881718.1	–
Eurotiomycetidae					
Arachnomycetales					
Arachnomycetaceae	*Arachnomyces minimus*	CBS 324.70 T	–	NG056963.1	AJ315167.1
	Arachnomyces nodosetosus	CCF 3975	HM205102.1	HM205103.1	HM205104.1
Eurotiales					
Aspergillaceae	*Aspergillus inflatus*	CBS 575.70A	MH859856.1	MH871635.1	–
	Hamigera avellanea	CBS 295.48 T	NR156333.1	–	NG061105.1
	Hamigera striata	CBS 377.48 T	MH856405.1	MH867954.1	–
	Leiothecium ellipsoideum	CBS 147.75	MH860904.1	MH872639.1	–
	Penicillium crustosum	DAOM 215345	JN942857.1	JN938953.1	JN939046.1
Thermoascaceae	*Byssochlamys nivea*	CBS 100.11 NT	NR144910.1	NG058631.1	NG061072.1

(Continues)

TABLE 1 (Continued)

Taxonomic position	Species	Isolate	GenBank accession no.		
			ITS	nucLSU	nucSSU
	Thermoascus crustaceus	CBS 181.67 ^{T}	NR144915.1	NG064060.1	NG062804.1
Trichocomaceae	*Rasamsonia emersonii*	CBS 266.71	MH860109.1	MH871885.1	—
	Sagenomella griseoviridis	CBS 470.78 ^{T}	MH861167.1	MH872930.1	—
	Talaromyces islandicus	CBS 126825	MH864247.1	MH875699.1	—
Onygenales					
Arthrodermataceae	*Arthroderma ciferrii*	CBS 272.66 ^{iT}	NR144888.1	NG057027.1	NG062604.1
	Arthroderma curreyi	CBS 138.26	KT155805.1	AY176726.1	AJ315165.1
	Ctenomyces serratus	CBS 187.61 ^{NT}	NR144890.1	NG058765.1	NG062605.1
Eremascaceae	*Eremascus albus*	CBS 975.69	MH859498.1	MH871279.1	FJ358348.1
Gymnoascaceae	*Amauroascus verrucosus*	NFCCI 2672 ^{T}	NR160558.1	JQ517293.1	JQ517294.1
	Gymnoascus reesii	CBS 410.72	MH860507.1	AY176749.1	GU733366.1
Onygenaceae	*Onygena corvina*	CBS 225.60	MH857958.1	MH869510.1	—
	O. corvina	CBS 281.48	—	FJ358287.1	FJ358352.1
Mycocaliciomycetidae					
Mycocaliciales					
Mycocaliciaceae	*Brunneocarpos banksiae*	CBS 141465 ^{T}	NR147648.1	MH878228.1	—
	Chaenothecopsis diabolica	H Tuovila 06-035 ^{PT}	NR120164.1	JX119118.1	—
	Chaenothecopsis golubkovae	Titov 6707 (UPS)	AY795859.1	AY795996.1	—
	Chaenothecopsis sitchensis	HT22	—	KF157988.1	KF157976.1
	Mycocalicium subtile	Wedin 6889 (UPS)	—	AY853379.1	—
	Phaeocalicium polyporaeum	ZW-Geo60-Clark	AY789363.1	AY789362.1	AY789361.1
Sclerococcomycetidae					
Sclerococcales					
Dactylosporaceae	*Rhopalophora clavispora*	CBS 637.73 ^{T}	NR152542.1	KX537757.1	NG061246.1
	Sclerococcum vrijmoediae	NTOU4002 ^{T}	KJ958534.1	KC692153.1	KC692152.1
Lecanoromycetes					
Acarosporomycetidae					
Acarosporales					
Acarosporaceae	*Sarcogyne plicata*	AFTOL-ID 4830	—	KJ766657.1	KJ766791.1
Lecanoromycetidae					
Caliciales					
Caliciaceae	*Calicium glaucellum*	Tibell 22319 (UPS)	AY450569.1	AY453646.1	—
	Calicium salicinum	CBS 100898	—	KF157982.1	KF157970.1

Note: Sequences generated in this study are in bold. ^{T} Sequence from type material; ^{ET} sequence from ex-type culture; ^{NT} sequence from neotype culture; ^{eT} sequence from epitype; ^{iT} sequence from isotype; ^{PT} sequence from paratype. Designation of cultures and culture collections: AFTOL-ID, Assembling the Fungal Tree of Life (AFTOL) project (www.lutzonilab.net/aftol); ARW, personal number of Alan Wood, ARC-Plant Protection Research Institute, South Africa; CBS, Centraalbureau voor Schimmelcultures, Netherlands; CCF, Culture Collection of Fungi, Department of Botany, Charles University in Prague, Czech Republic; Clark, Clark University, USA; CMW, Forestry and Agricultural Biotechnology Institute, University of Pretoria, South Africa; COAD, Coleção Octávio de Almeida Drumond, Universidade Federal de Viçosa, Brazil, CPC, Culture collection of Pedro Crous, housed at CBS, Netherlands; DAOM, Canadian National Mycological Herbarium, Ottawa Research and Development Centre, Canada; F, personal number of Zdenek Palice, Institute of Botany, Academy of Sciences of the Czech Republic; GFCC, Goa University Fungus Culture Collection and Research Unit, India; H Tuovila, HT, personal number of Hanna Tuovila, University of Helsinki, Finland; MA, Real Jardín Botánico, Spain; MUCL, Mycotheque de l'Universite Catholique de Louvain, Belgium; NFCCI, National Fungal Culture Collection of India, India; NTOU, National Museum of Natural Science Herbarium, Taiwan; PREM, National Collection of Fungi, South Africa; UPS, Museum of Evolution, Sweden.

measuring the angle of discoloured tissue with ImageJ software (https://imagej.nih.gov/ij/index.html) using the circumference of the branch pith as the reference centre point. The captured data were analysed statistically using R software by performing analysis of variance (ANOVA) and posterior Tukey's test (HSD) for each kind of measurement individually.

Reisolations were made from lesion margins of all inoculated branches including control treatments. For this purpose, the lesions were surface disinfested with 70% ethanol (10 s), followed by 5% sodium hypochlorite (1 min), and then cleaned with sterile distilled water. Small segments were cut from the leading edges of the lesions and incubated in Petri dishes containing 50% PDA for 7–14 days. The identification of the emerging isolates was confirmed by sequencing of the ITS region.

3 | RESULTS

3.1 | Monitoring of disease symptoms

Decline symptoms were observed on *Araucaria* trees of all ages, including young seedlings, at all four sites assessed. The predominant symptom observed was a progressive death of branches (Figure 2a,b) starting most frequently from the base of the crown and occasionally moving laterally. Whole branches or parts of trees were observed yellowing from mid-November and throughout December and January (spring to summer). Most of these tree parts had died by the middle of February, but branches continued to die up to April. After 1–2 years, the dead leaves had fallen, with the dry medulla remaining. Girdling cankers were consistently associated with dying branches of most diseased trees at the sites on the Andes mountain range, but these were rarely found on trees on the coastal range (Trongol Alto in Nahuelbuta). A low incidence of branches infested by insects and by secondary leaf pathogens were consistently observed in all sites.

Cankers on the Andean *Araucaria* populations were found on trees of all ages, on branches of different sizes and in some cases on the main stems of a large proportion of the trees. In addition, at the same sites, most of the branches that had recently died exhibited a canker near or directly at its base. Monitoring of specific lesions for a 2-year period provided clear evidence that the cankers resulted in branch death. Variability in the rate of spread of the discolouration and the production of secondary symptoms was observed in lesions that were tracked over time. Freshly developing cankers were observed on trees growing at all the sites inspected in the Andes at all three times of inspection (November and December in 2017, 2018, and 2019). This showed that infection could occur between the end of winter (August) and the beginning of spring (September–October).

Initial infections included reddish-brown areas of discolouration, approximately 3 mm long at the bases of individual isolated leaves, which in most cases were chlorotic or dead (Figure 3a). As infection progressed it caused slight swelling of the tissues leading to small cracks that exuded copious amounts of resin. The infection continued to spread at the base of the leaves, both longitudinally and laterally, resulting in the death of attached leaves in a ring-like pattern (Figures 2c,d and 3b,c). Over time, cankers that had developed in these rings of infection became darker and cracks coalesced into larger lesions. After 1–2 years, cankers had girdled the branches and the leaves distal to these cankers became chlorotic and died (Figures 2d and 3c). Cankers were more often found at the bases of branches (Figure 2e) and/or secondary branches and these consistently led to the death of the distal portions of those branches. Cankers were also observed in the middle of secondary branches, which resulted in the death of either the distal portion or entire secondary branch. Similar cankers were observed on the trunks of young trees (Figure 2h), and, in some cases, these resulted in the death of tree parts above those cankers.

3.2 | Collection of samples and isolation of fungi

Fresh and well-developed cankers were easily collected from all three sites visited in the Andes mountain range, and these consistently displayed tissue discolouration and resin exudation. However, cankers found in Trongol Alto (Nahuelbuta, Coast range), which had a drier appearance, were scarce, including some sample collection points where no cankers were found. In such cases, samples of branch segments that contained small areas of brownish red discolouration at the base of one to three leaves were collected.

Many different fungi were obtained in the primary isolations from the margins of lesions of samples from all sites. Most were recovered only once or at low frequency. Based on culture morphology, only a single fungus was consistently recovered from branch and stem cankers. These were also only from samples collected from sites in the Andes mountain range. No dominant fungal morphotype was recovered from samples collected at the Coastal range site (Trongol Alto, Nahuelbuta).

The main morphotype recovered from cankers from the sites in the Andes mountain range was a pale white colony, with radial aerial mycelium that grew slowly on the PDA, reaching 25 mm diameter after 14 days at 20 °C. A total of 49 isolates of this dominant fungal morphotype were obtained from branch cankers and 11 were obtained from cankers on the main stems of trees. Additionally, 14 isolates of an identical morphotype were obtained from the single spore isolations made from 14 different ascocarps collected from four different cankers.

3.3 | Phylogenetic analysis

Isolates representing the dominant morphotype obtained by isolation from lesion margins and from fruiting bodies found on cankers had identical ITS sequences. BLAST searches with these sequences had the highest identity to species of *Caliciopsis*. This was consistent with expectation due to the morphology of the fruiting bodies from which isolations were made. The closest matches were *Caliciopsis calicioides* (acc. no. JX968549.1) with only 86.36% identity, *Caliciopsis indica* (acc. no. NR_119752.1) with 86.01% identity, and *Caliciopsis eucalypti* (acc. no. NR_154836.1) with 85.08% identity.

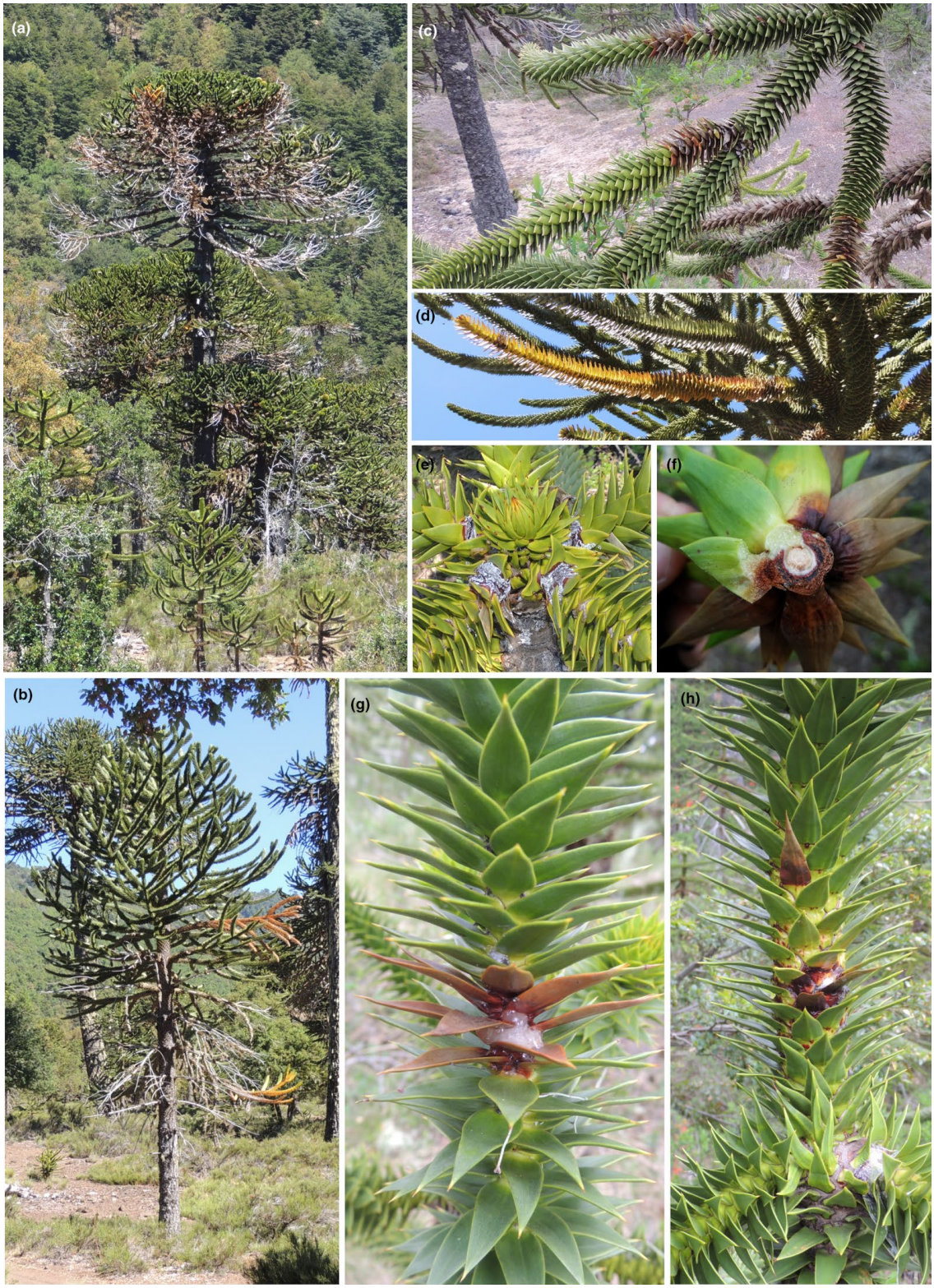

FIGURE 2 Symptoms of canker disease observed on *Araucaria araucana*. (a,b) Adult and young trees showing progressive death of branches; (c,d) ring-shaped cankers on branches; (e) cankers on the bases of branches; (f) transverse cut of young branch canker showing girdling of the phloem; (g) fresh canker with exudation of resin; (h) fresh canker on main trunk of a young tree

Three isolates of the dominant morphotype were included in the data sets with sequences obtained from GenBank for phylogenetic analyses. When aligned, these resulted in a total of 45 taxa for the ITS gene region, 50 for the nucLSU gene region, 28 for the nucSSU gene region, and 56 taxa for the combined data set. Maximum-likelihood and Bayesian-inference analyses using the individual

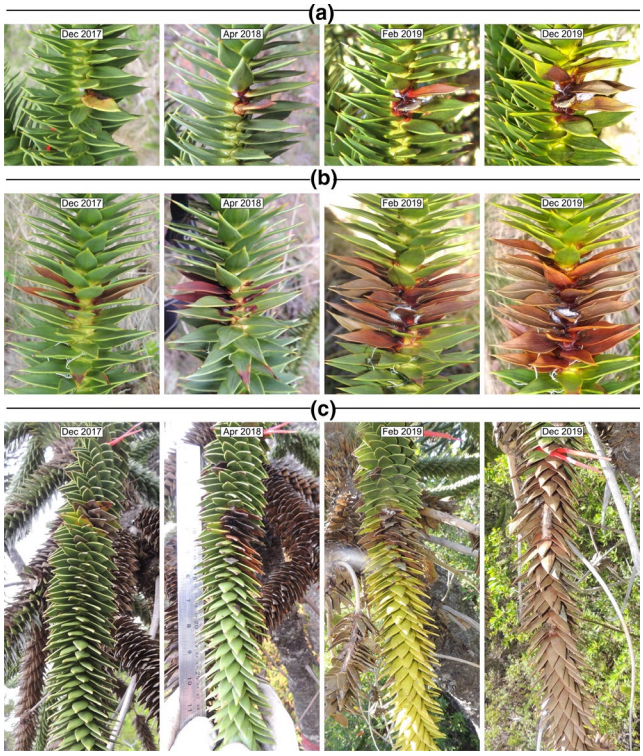

FIGURE 3 Long-term symptom progression of canker disease on three branches of *Araucaria araucana* over a two-year period from December 2017 to December 2019. (a) Initial stage of infection starting from one diseased leaf; (b) intermediate stage of infection including complete girdling; (c) advanced stages of infection with the appearance of secondary symptoms and death of branches

(Figures S1, S2 and S3) as well as the combined gene region (Figure 4) consistently grouped the isolates in an independent clade at the base of the Coryneliaceae family. This supported a conclusion that the fungus represented a novel genus. High branch support (bootstrap above 95%) was obtained for most nodes in the Coryneliaceae clade in phylogenetic trees made for all data sets. Results obtained with the ITS, nucLSU, and the combined data sets consistently separated *Caliciopsis* from *Hypsotheca* and showed that *Caliciopsis* is paraphyletic. However, ITS and nucLSU trees were not consistent in the position of species belonging to other genera in Coryneliaceae (*Corynelia*, *Lagenulopsis*, and *Tripospora*), placing them in a single clade sister to either *Hypsotheca* or *Caliciopsis*, respectively.

3.4 | Morphology

Ascocarps were only observed in cankers and these structures were never found in culture. These were also the most commonly occurring and obvious fruiting structures found on cankers (Figure 5e–h), and were most often found around and/or inside cracks in the bases of the leaves (Figure 5m). Ascocarps were black straight or tilted column-like structures with an ascigerous swelling, most commonly in the middle and tending to an upper position closer to the apex, bearing a reddish-brown mass of spores (mazaedium) at their tips. Asci were long, pedicellate and bearing eight reddish-brown ascospores with verrucose ornamentation (only seen at high amplification; Figure 5i–l). Spermogonia were identified from observing the ascocarps in development (Figure 5d,e); these emerged subepidermally from the base of diseased leaves (Figure 5a–d) in several samples. Spermatia obtained from the spermogonia on cankers were hyaline and obtuse or ovoid (Figure 5c). Ascocarps developed from the same stroma as the emerging spermogonia. Cultures in MEA were white when young, mostly submerged, with little aerial mycelium growing radially and turned darker with time, producing a hazel to umber brown colour. Some cultures produced spermogonia from young mycelium at the edge of the colonies, forming a concentric halo in the centre, while in other cultures they only formed at the margins when older.

3.5 | Taxonomy

Results of the phylogenetic analyses carried out for the most commonly encountered morphotype did not identify this fungus as any species for which sequence data were available. The fungus resided outside of the clade representing the genus *Caliciopsis* and in a clade of its own. Additionally, the results of morphological analyses indicated that the set of characters for the fungus isolated in this study were unique and different from *Caliciopsis* species described on *Araucaria* trees from Chile. Based on its unique morphology and phylogenetic placement, this fungus is described in a novel genus and species, as follows:

3.5.1 | *Pewenomyces* Balocchi, I. Barnes & M. J. Wingf gen. nov.

MycoBank MB834914

Etymology: From “pewen”, the name of *Araucaria* in the Mapudungun, language of the native Chilean and Argentinian Mapuche culture.

Type species: *Pewenomyces kutranfy* Balocchi, I. Barnes & M.J. Wingf

Ascomata Individually or gregarious, arising individually or in pairs from a subepidermal stroma that may or may not erupt and become evident. Black in colour, ventricose, sometimes straight but most commonly tilted, ascigerous swelling position variable, mostly subapical to medium but also submedian, rarely collapsed to one side, very rarely branched. A powdery reddish-brown mass of mature ascospores accumulate on tip of mature ascomata. Ascomal wall of *textura porrecta* to *textura prismática*, interior *textura intricata*. *Asci* containing 8 spores, spathulate, ovoid to ellipsoid in spore bearing part, with a long and slender stipe, deliquescent. *Ascospores* reddish brown, thick-walled, mostly globose, but some ovoid to ellipsoid, verrucose. *Spermogonia* gregarious, erupting from plant tissue, black in colour, globose or piriform at maturity, creamy white spore exudation coming from an ostiole when mature. *Spermatia* hyaline, asymmetric, oblong, ovoid or reniform, aseptate, smooth.

Notes. *Pewenomyces* ascomatal morphology and arrangements are more similar to those of *Hypsotheca* and *Caliciopsis* than

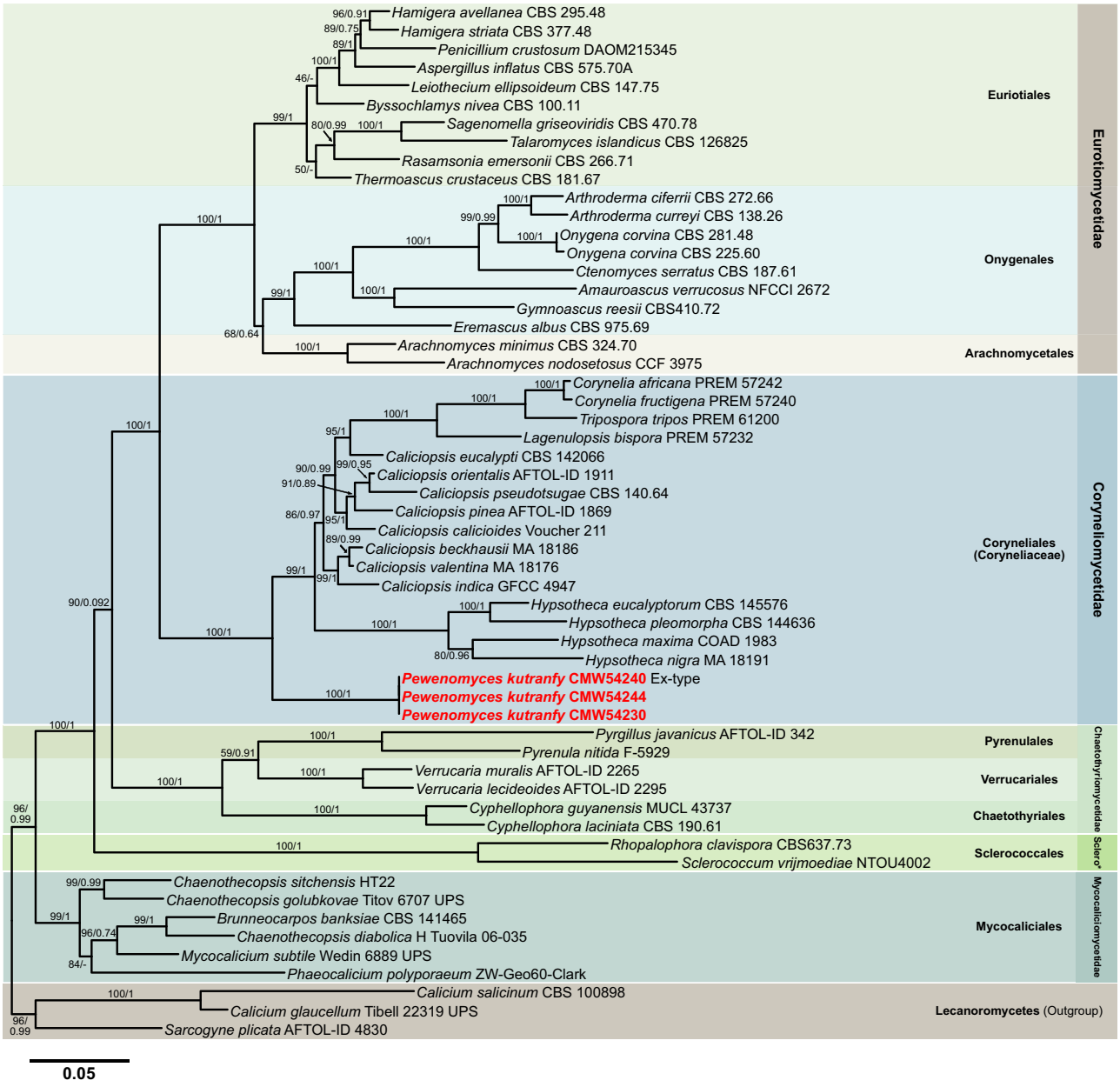

FIGURE 4 Maximum-likelihood phylogenetic tree for the concatenated nucSSU, ITS, and nucLSU gene sequences for the subclasses and part of the subsequent orders within Eurotiomycetes. The new taxon (in red) is located independently at the base of the subclass Coryneliomycetidae (monotypic: order Coryneliales, also monotypic: family Coryneliaceae). Numbers on branches correspond to bootstrap values (n = 1,000) and posterior probabilities values from Bayesian inference, respectively. *: Sclerococcomycetales

to other genera in the Coryneliaceae. Ascomatal characteristics and dimensions have typically been used to separate genera in Coryneliaceae, and the existence of a stipe under the ascigerous swelling has been seen as the diagnostic morphological feature for *Caliciopsis* (Fitzpatrick, 1942b). More recently, the existence of a stipe has emerged as a common feature of *Caliciopsis*, *Hypsotheca*, and *Pewenomyces*, separating these three genera from the rest of the family. As a consequence, the existence of a stipe in *Pewenomyces* ascocarps serves as evidence that this genus does not reside with the remaining and unsequenced genera of the Coryneliaceae, that is, *Coryneliospora*, *Coryneliopsis*, *Coryneliella*, and *Fitzpatrickella* (Benny et al., 1985a, 1985b; Fitzpatrick, 1942a).

3.5.2 | *Pewenomyces kutranfy* Balocchi, I. Barnes & M. J. Wingf sp. nov. (Figures 5 and 6)

MycoBank MB834915

Etymology: From indigenous Chilean and Argentinian Mapuche language mapudungun; “kutran”, meaning a disease and the “-fy”,

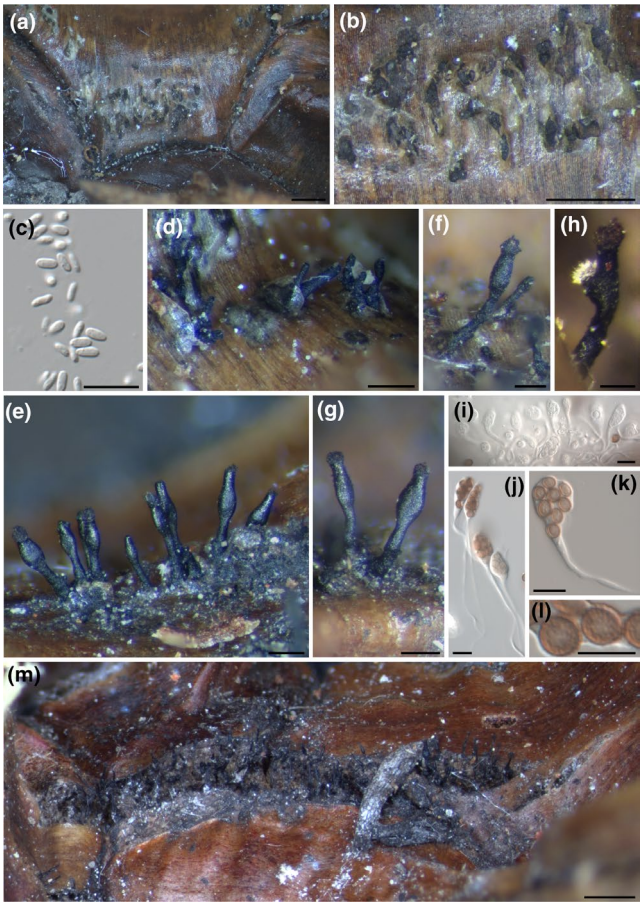

FIGURE 5 Fruiting bodies on branch cankers of *Araucaria araucana*. (a,b) Asexual stage (spermogonia) erupting subepidermally; (c) spermatia; (d,e) ascomata developing from stroma of spermogonia; (f,g) mature ascomata; (h) ascomata bearing a lateral spermogonia; (i,j) immature asci; (k) mature ascus bearing mature ascospores; (l) ascospores showing verrucose ornamentation; (m) ascomata's habit on cracks on base of the leaves. Scale bars: a, b, m = 1 mm; d, f, h = 0.1 mm; e, g = 0.2 mm; c, i–l = 10 μm

suffix from Latin "-ficare", to "make into". Thus, illustrating the fact that the fungus causes disease.

Ascomata Individual or gregarious, emerging from cracks at the base of leaves and stems. Black in colour, elongate, ventricose with a submedian to supramedian ascigerous swelling, (358) 473 ± 91 (600) μm tall, (122) 148 ± 23 (173) μm wide in the broadest part and (83) 103 ± 18.3 (126) μm at the tip. Ascomal wall composed of a few layers of dark *textura porrecta* cells and hyaline cells of *textura prismatica*, centre of *textura intricata*. *Asci* spathulate, long stalked (pedicellate), eight-spored, (13) 15.8 ± 1.7 (22) μm long and (8) 10.2 ± 0.7 (11) μm wide in spore-bearing part. *Ascospores* reddish brown, thick walled, verrucose, mostly globose or subglobose, rarely ellipsoidal, (4.0) 4.7 ± 0.5 (6.4) μm long and (3.4) 4.3 ± 0.5 (5.3) μm wide. *Spermogonia* erupting from plant tissue, at base of affected leaves, spherical to obpyriform, exuding a small white semitranslucent drop of spores. *Spermatia* hyaline, oblong, ovoid, or reniform (2.5) 3.6 ± 0.6 (4.6) long and (1.1) 1.3 ± 0.2 (1.7) wide.

Culture characters: Slow growing cultures variable in morphology. Optimum temperature for growth between 15 and 20 °C reaching 32–35 mm after 28 days in MEA and 24–27 mm on oatmeal agar (OMA; Figure 6). Faster growth observed at 5 and 10 °C than at 25 °C. No growth seen at 30 or 35 °C after 28 days on any tested culture medium. Cultures at 35 °C failed to grow when plates were returned to 20 °C for 14 days, indicating these high temperatures result in their death. Cultures on MEA and incubated at 20 °C were white when young, mostly submerged, with little aerial mycelium, growing radially, with a saffron white to light hazel brown colour underneath. Cultures gradually becoming darker and hazel to umber brown in colour, some with saffron to buff grey aerial mycelium at the centre. The reverse side of plates dark, especially at the edges, with a hazel brown to sepia colour. Fully grown cultures flat, round, with either entire or curled margins. Cultures on OMA white, sunken, with aerial mycelium absent or very minimally present, growing sparsely with curled margins. On reverse, cultures white, becoming creamy coloured with time.

Spermogonia were inconsistently observed, only in MEA, and occurred more frequently at lower temperatures (5–15 °C). Produced from the young mycelium at the edges of the colonies, forming a concentric halo at the centre or edge of the colony depending on when they are developed. Gregarious or in clusters, obpyriform to spherical when solitary, dark brown to black with a milky white to yellowish spore mazaedium in the top when mature. Spermatia are hyaline, aseptate, shape varies from symmetrical oblong to reniform to asymmetrical obovoid with an apparent constriction in the middle, (3.1) 5.6 ± 1.1 (8.8) μm long and (1.4) 2.1 ± 0.5 (3.4) μm wide.

Substrate: Cankers on branches of *Araucaria araucana*

Specimens examined: Chile, Araucanía (IX), Villarrica National Park sector Puesco, 13 December 2017, Felipe Balocchi, HOLOTYPE PREM 63075 (dried culture), ex-type culture CBS 146709 = CMW54240 = AR128 (isolated from lesion margins of cankers on branches of *Araucaria araucana*), GenBank: ITS = MT334515, nucLSU = MT334521, nucSSU = MT359913; PARATYPE PREM 63077 (dried culture), ex-type culture CBS 146711 = CMW54244 = AR161 (isolated from lesion margins of cankers on branches of *Araucaria araucana*), GenBank: ITS = MT334515, nucLSU = MT334521, nucSSU = MT359913. Chile, Araucanía (IX), Conguillío National Park sector Los Paraguas, 11 December 2017, Felipe Balocchi, PARATYPE PREM 63076 (dried culture), ex-type culture CBS 146710 = CMW54230 = AR050 (isolated from lesion margins of cankers on branches of *Araucaria araucana*), GenBank: ITS = MT334514, nucLSU = MT334519, nucSSU = MT359912. Chile, Biobío (VIII), Ralco National Reserve, from cankers in the branches of *Araucaria araucana*, 28 December 2017, Felipe Balocchi, living culture CMW54251 = AR221 (isolated from lesion margins of cankers on branches of *Araucaria araucana*).

Notes. Although *P. kutranfy* described here resides in a novel monotypic genus, it was relevant to compare its morphology with *Caliciopsis* species described previously from *A. araucana* (Butin, 1970). In this regard, ascomata were more similar in size to

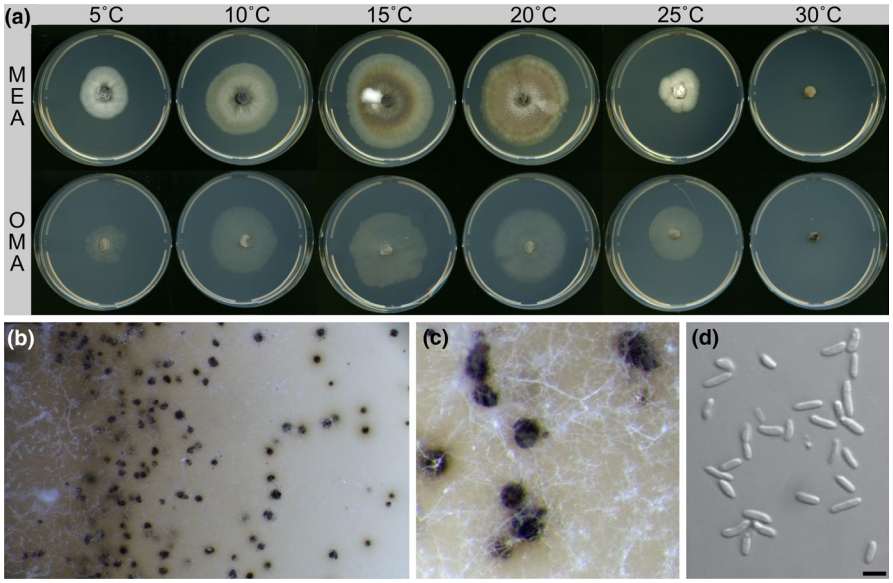

FIGURE 6 Culture characteristics of *Pewenomyces kutranfy* isolate CMW54240. (a) Culture growth after 28 days at six temperatures and two culture media: malt extract agar (MEA) and oatmeal agar (OMA); (b,c) fruiting bodies (spermogonia) on cultures on MEA; (d) spermatia. Scale bar: 5 μm

TABLE 2 Comparison of morphological characteristics of *Caliciopsis* species and *Pewenomyces kutranfy* on *Araucaria araucana*

Structure	Character	*Caliciopsis brevipes*[a,b]	*Caliciopsis cochlearis*[a,b]	*Pewenomyces kutranfy*
Ascomata	Height (μm)	600–1,000	350–700	358–600 (473 ± 91)
	Width (μm)	200–280	80–140	122–173 (148 ± 23)
	Tip width (μm)	100–160	50–75	83–126 (103 ± 18)
Asci	Length (μm)	18–22	16–18	13–22 (15.8 ± 1.7)
	Width (μm)	8–10	10–14	8–11 (10.2 ± 0.6)
Ascospores	Length (μm)	5.6–7.0	4.5–5.5	4.0–6.4 (4.7 ± 0.5)
	Width (μm)	4.5–6.0	4.0–4.6	3.4–5.3 (4.3 ± 0.5)
Spermogonia	Height (μm)	140–250	100–200	NA
	Width (μm)	140–250	NA	100
Spermatia	Length (μm)	4.2–5.5	3.2–4.2	2.5–4.6
	Width (μm)	2.0–3.0	1.0–1.5	1.1–1.7
	Shape	Allantoid/ellipsoidal	Allantoid	Oblong/ovoid

Abbreviation: NA, not available.

[a]Butin (1970).

[b]Benny et al. (1985b).

C. cochlearis than to those of *C. brevipes* (Table 2). Most features were found to be more variable than reported in literature, even for some previously considered diagnostic features such as the position of the ascigerous swelling. Although the ascomata on the cankers most commonly had a subapical ascigerous swelling (similar to those found in *C. cochlearis*), several ascocarps had a median to submedian swelling (similar to *C. brevipes*). The ascocarps were similar to those of *C. cochlearis* in height, but ascocarps on cankers were wider and the subepidermally erupting stromata remained visible at the base of most ascocarps. This was in contrast to those in *C. cochlearis* where ascocarps appear to erupt directly from the plant tissue. Dimensions of asci and ascospores obtained from ascocarps on cankers were also more variable than those described for *C. brevipes* and *C. cochlearis*. Although ascospore dimensions were most similar to those of *C. cochlearis*, those found in *P. kutranfy* were slightly larger. Spermatia obtained from spermogonia on cankers were shorter and wider than any of the two *Caliciopsis* species mentioned above; rather than being allantoid shape, they were mostly ovoid to obtuse.

3.6 | Pathogenicity

Six weeks after inoculation, distinct lesions had developed on all branches inoculated with the two isolates of *P. kutranfy*. All the infected branches had copious resin exudation covering the point of inoculation and a red-brown discolouration was observed spreading to the bases of the attached leaves (Figure 7). Removal of the outer layers of plant tissue exposed the longitudinal and lateral spread of the discolouration, and cutting the lesions transversely exposed the spreading of the discolouration through the phloem, reaching the cambium, and

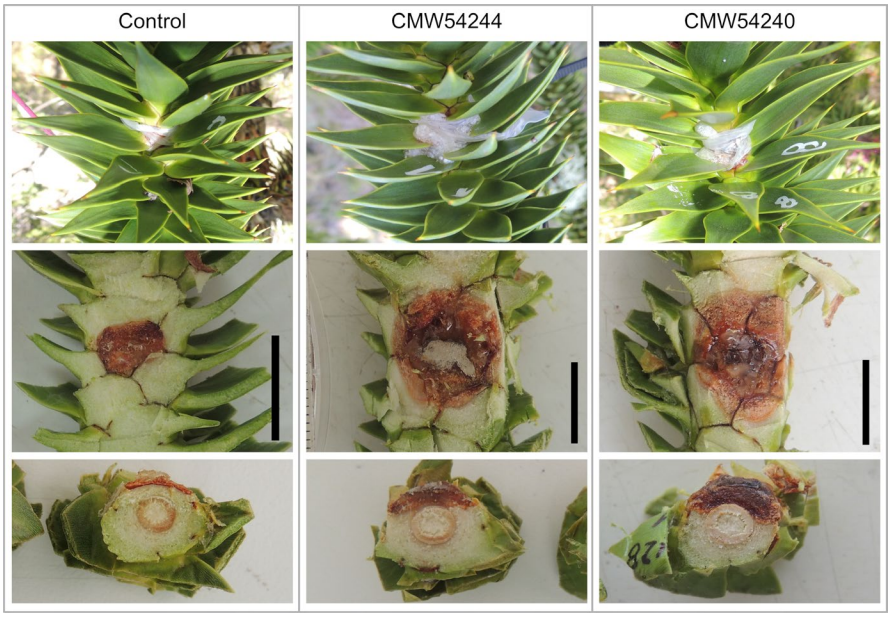

FIGURE 7 Results of inoculations with two isolates of *Pewenomyces kutranfy* and a control treatment on branches of *Araucaria araucana* after 6 weeks, showing differences in resin exudation (top), discolouration (middle), and girdling the branch (below). Scale bars: 10 mm

girdling the branch. Lesions produced by the isolate CMW54240 were 13.2 ± 2.4 mm long and had girdled 44 ± 3.3% of the branch circumference while isolate CMW54244 produced lesions 12.4 ± 2.5 mm long and girdled 41.2 ± 4.8% of the branch circumference. Differences between lesion sizes and girdling percentages produced with the two isolates were not significant according to Tukey's test ($p < .05$) (Figure S4).

In contrast, none of the control branches had resin exudation and were free of discolouration other than at the surface of the wound, which became dry. The size of the wounds remained the same as the initial inoculation wounds, which were 7.3 ± 1.4 mm long and the wound shape was the same as the initial leaf-base. When the outer tissues were removed, no discolouration was found in any of the inoculated branches. Cutting lesions transversally showed no signs of infection in the phloem, only a superficial layer of dry cells, which in circumference covered only 30.9 ± 2.8%. Lesion size and girdling percentage of both isolates of *P. kutranfy* were significantly different with those of the control.

Reisolations from the lesion margins resulted in 100% recovery of the inoculated fungus, while isolations from the control treatments yielded only contaminant fungi.

4 | DISCUSSION

The results of this study showed that an aggressive canker disease is directly related to branch die-back and decline of *A. araucana* trees in the main distribution of these trees in the Chilean Andes. A previously unidentified fungus in the Coryneliaceae was consistently associated with these cankers. Based on phylogenetic inference and supported by morphological characteristics, the fungus is described here in the new genus *Pewenomyces* as *P. kutranfy*. In field pathogenicity tests, *P. kutranfy* was shown to cause cankers similar to those observed under natural conditions.

Pewenomyces is most similar morphologically to *Caliciopsis* and to *Hypsotheca*, two genera that have similar morphological characters. The genus *Hypsotheca* was resurrected by Crous et al. (2019) to relocate three *Caliciopsis* species, based mainly on DNA sequence data. Those authors showed that species of *Caliciopsis* that had not had their identity confirmed by DNA sequence data might not actually belong to the genus, and thus, their morphology may not be representative of the genus. If only the nine species confirmed as *Caliciopsis* by sequence data are taken into account (Table 3), the common morphological traits are ascomata over 1 mm tall (except for *C. indica* and *C. moriondi*), with the ascigerous swelling terminal to subterminal (except *C. calicioides*), ascospores ellipsoidal to subglobose or ovoid (except *C. indica*) with smooth walls (Fitzpatrick, 1942b; Garrido-Benavent & Pérez-Ortega, 2015; Migliorini et al., 2020; Pratibha et al., 2010). Because the genus *Hypsotheca* has only recently been resurrected and one of its species, *Hypsotheca eucalyptorum*, was described only from culture, the description of morphological characteristics for this genus is limited, especially regarding the sexual morph. Observations of the ascomata of three sequenced species appear to show that these species form smaller fruiting bodies with the ascigerous swelling at a lower position (median or submedian, with the exception of *H. maxima*). However, both *Caliciopsis* and *Hypsotheca* include species that do not conform to these characteristics, which limits them as diagnostic features. It is also noted that morphological differences between these genera and *Pewenomyces* described in the present study are scarce; *Hypsotheca* species produce a hyphomycete state in cultures (Crous et al., 2019), which has not been reported for any *Caliciopsis* species and was not found in *Pewenomyces*. Furthermore, *P. kutranfy* produces ornamented (verrucose) ascospores rather than the smooth-walled ascospores in *Caliciopsis*, or the foveolate ornamentation seen in *Hypsotheca*.

The morphology of *P. kutranfy* was unlike that of either of the two *Caliciopsis* species (*C. brevipes* and *C. cochlearis)* described on *A. araucana* by Butin (1970). Even though neither of these species

TABLE 3 Main morphological characters for the species confirmed by sequencing as *Caliciopsis* and *Hypsotheca*

	Ascomatal dimensions				Asci	Ascospores			Spermogonia	Spermatia	
Species	Stroma	Height (μm)	Diameter (μm)	Ascigerous swelling	Dimensions (μm)	Ornamentation	Shape	Dimensions (μm)	Diameter (μm)	Shape	Dimensions (μm)
Caliciopsis beckhausii[g]	Absent	(500) 700–1,100 (1,500)	(75) 90–130 (160)	Median tending to subterminal	15–21 × 7–10	Smooth	Globose to subglobose (ellipsoidal)	(5.4) 6.4–8.4 (11) × (4.8) 5.7–7.5 (10)	65–150 (250)	Subcylindrical to allantoid	(3.5) 3.9–4.5 (4.7) × (1.2) 1.3–1.7
C. calicioides[a,d]	Present	1,400–1,800	200–340	Median or submedian	15–20 × 8–11	Smooth	Subfusiform to ellipsoidal (oval)	(6) 7 (10) × 3.5 (5)	140	—	2.5–3.0
C. eucalypti[b]	—	—	—	—	—	—	—	—	150–200	Bean-shaped obtuse ends	3–4 × 1.5
C. indica[k]	Absent	205–300	35–70	Terminal	18–28 × 4–7	Smooth	Globose	2.5 – 4.5 (Ø)	—	—	—
C. moriondi[i]	Present	(450) 821–869 (1,240)	(81) 137–147 (268)	Terminal	12.0–14.2 × 5.3–7.4	—	Subglobose to ellipsoidal	(3) 4.4 (6.2) × (1.8) 2.5 (3.5)	—	Slightly fusiform	—
C. orientalis[f]	—	2,000	150–200	Subterminal	16–19 × 7–9	—	Ellipsoidal	4.5–6 × 3.5–4.5	100–200	Allantoid	3.5 × 1.0
C. pinea[d,f,h]	Present	500–1,000	175–275	Terminal	12–17 × 5–8	—	Ellipsoidal to ovoidal or globose	3.5–6 × 2–4	100–150	Rod-shaped to allantoid	2.5–3.5 × 1.0
C. pseudotsugae[f]	—	1,000–3,000	250	—	12–19 × 5–9	—	Ellipsoidal to subglobose	(3) 4–5 (6) × 2–4	40–140	Allantoid	3.5–5.0 × 1.0–1.5
C. valentina[g]	Present	(600) 700–1,100 (5,000)	(100) 115–145 (160)	Subterminal	20–35 × 6–10	Smooth	Subglobose to ellipsoidal	(5.3) 6.2–7.8 (9.6) × (4) 5.0–6.4 (8)	120–170	Subcylindrical to allantoid	(4) 4.2–4.8 (5) × (1) 1.2–1.6
Hypsotheca eucalyptorum[c,l]	—	—	—	—	—	—	—	—	180–200	Subcylindrical with obtuse ends	(3) 3.5–4.0 (4.5) × 1.5 (2)
H. maxima[d]	Present	1,000–1,500	125–150	Median tending to subterminal	15–17 × 10	—	Globose, subglobose	5–6 × 4–5	—	Narrow-fusiform	11–24 × 4
H. nigra[a,e]	Present	≤500	170–24	Usually basal, submedian	—	Foveolate	—	4–5 (Ø)	—	—	—
H. pleomorpha[j]	Absent	250–700 (900)	65–130	Submedian to suprabasal	10–13 × 7–8	Smooth	Depressed globose to subellipsoid	3.3–3.7 (Ø)	80–150	Oblong to allantoid	3–5 × 1–2

Note: (Ø) for ascospore dimensions indicates that measurement of only a single dimension is provided.

[a]Benny et al. (1985b).

[b]Crous et al. (2016).

[c]Crous et al. (2019).

[d]Fitzpatrick (1920).

[e]Fitzpatrick (1942b).

[f]Funk (1963).

[g]Garrido-Benavent and Pérez-Ortega (2015).

[h]McCormack (1936).

[i]Migliorini et al. (2020).

[j]Pascoe et al. (2018).

[k]Pratibha et al. (2010).

[l]Described only from colonies in culture medium.

was reported to cause cankers, our initial hypothesis was that *P. kutranfy* might represent one of them based on general morphological characteristics and the niche in which these fungi occur. However, *C. brevipes* and *C. cochlearis* are more similar to each other than to any other *Caliciopsis* species and share some common features not seen in any other *Caliciopsis* species, such as verrucose ornamentation of the ascospores (Benny et al., 1985b). Taking into consideration the fact that DNA sequence data for some originally described *Caliciopsis* species has resulted in placing them in a different genus, it is reasonable to expect that Butin's species most likely reside in *Pewenomyces* rather than in *Caliciopsis*. Resolving this question must await collections from *A. araucana* that fit morphological characteristics of *C. brevipes* and *C. cochlearis* and from which cultures can be made.

Pathogenicity tests in this study showed that *P. kutranfy* is able to cause cankers similar to those found in the field and is thus considered as a new canker pathogen in the Coryneliaceae. This family of fungi is emerging as an important group of tree pathogens. It now includes a group of *Caliciopsis* species known to cause cankers on several conifer species, such as *C. morindi* (Migliorini et al., 2020) and *Caliciopsis pinea* on *Pinus* spp., *Caliciopsis pseudotsugae* on Douglas-fir (*Pseudotsuga* spp.) and *Caliciopsis orientalis* on *Tsuga* spp. (Funk, 1963). In addition, there are two *Hypsotheca* species, including *Hypsotheca nigra* that causes galls on twigs of different *Juniperus* spp. and *Hypsotheca pleomorpha* causing cankers on different *Eucalyptus* species (Pascoe et al., 2018). Among these, Caliciopsis canker disease on *Pinus strobus* caused by *C. pinea* in the USA (Munck et al., 2015) and the canker disease caused by *H. pleomorpha* on *Eucalyptus* spp. in Australia, have resulted in recent outbreaks of diseases on both planted and natural forests. This would be similar to the canker disease caused by *P. kutranfy* described in the present study that occurs in natural *A. araucana* forests.

Culture growth studies with *P. kutranfy* showed that this fungus has a very evident tolerance to cold temperatures. This is consistent with its area of occurrence and suggests an adaptation to high elevations and extreme cold in winter that are typical of mountain ecosystems such as in the Andes (Diaz et al., 2003; Mellado-Mansilla et al., 2018). Other species in the Coryneliaceae have also been described from Chilean Andes environments (Butin, 1970; Fitzpatrick, 1942b; Léveillé, 1846), indicating that members of the Coryneliaceae may have been present in these environments for long periods of time.

Climate change could be among the drivers of the disease on *A. araucana* considered in this study. Weather conditions are known to have been outside of their usual range at the time when disease symptoms were first recorded on trees in the Chilean Andes. These conditions included an extended period of drought, referred to as the mega-drought of 2010–2018 (Garreaud et al., 2020), and a general increase in temperatures in the Andes mountain range at the same time (Schumacher et al., 2020). This led to the hypothesis that drought and/or extreme temperatures in summer resulted in stress to the trees, predisposing them to pest and pathogen damage. Although this scenario might in part explain the diversity of secondary agents found at all sites considered in this study, the fact that *P. kutranfy* grows poorly at temperatures above 20 °C is in conflict with the hypothesis that increased summer temperatures were responsible. In contrast, a rise in winter or early spring temperatures observed during the same period offer a more plausible explanation of the driver of canker disease. Higher temperatures in winter, especially at high elevations, would have a direct effect on fungal pathogens; for example, it would affect the survival of inoculum during winter as well as fungal biology, including reproduction and infection rates (Simler-Williamson et al., 2019).

The effect of climate change on forest pests and pathogens has become increasingly important in recent years. Changes in climatic conditions can affect the impact or emergence of diseases via diverse mechanisms (Ramsfield et al., 2016). Results of this study suggest that the emergence of the canker disease caused by *P. kutranfy* could be linked to a rise in winter temperatures. Such conditions could allow a native pathogen to cause damage not previously possible or facilitate the invasion process for an introduced pathogen. Although there is more evidence from this study to suggest that *P. kutranfy* is native to the environment in which it is causing disease, this question remains to be resolved.

ACKNOWLEDGEMENTS

The authors would like to acknowledge the funding bodies for this work, namely the Tree Protection Cooperative Programme (TPCP), the Forest and Agricultural Biotechnology Institute (FABI) and the University of Pretoria, South Africa, the Chilean National Forest Corporation (Corporación Nacional Forestal, CONAF), and Bioforest S.A. Arauco, Chile. We would also like to acknowledge the personnel of the phytosanitary division and laboratory technicians at Bioforest S.A. for their assistance in laboratory and field work.

CONFLICT OF INTEREST

The authors declare that they have no conflicts of interest.

DATA AVAILABILITY STATEMENT

The data that support the findings of this study are available from the corresponding author upon reasonable request.

ORCID

Felipe Balocchi https://orcid.org/0000-0003-4790-6283
Mike J. Wingfield https://orcid.org/0000-0001-9346-2009
Rodrigo Ahumada https://orcid.org/0000-0002-2397-2721
Irene Barnes https://orcid.org/0000-0002-4349-3402

REFERENCES

Barnes, I., Roux, J., Wingfield, M.J., Coetzee, M.P. & Wingfield, B.D. (2001) Characterization of *Seiridium* spp. associated with cypress canker based on β-tubulin and histone sequences. *Plant Disease*, 85, 317–321.

Benny, G.L., Samuelson, D.A. & Kimbrough, J.W. (1985a) Studies on the Coryneliales. I. *Fitzpatrickella*, a monotypic genus on the fruits of *Drimys*. *Botanical Gazette*, 146, 232–237.

Benny, G.L., Samuelson, D.A. & Kimbrough, J.W. (1985b) Studies on the Coryneliales. IV. *Caliciopsis*, *Coryneliopsis*, and *Coryneliospora*. *Botanical Gazette*, 146, 437–448.

Besoain, X., Guajardo, J. & Camps, R. (2017) First report of *Diplodia mutila* causing gummy canker in *Araucaria araucana* in Chile. *Plant Disease*, 101, 1328.

Butin, H. (1970) Zwei neue *Caliciopsis*-arten auf chilenischen koniferen. *Journal of Phytopathology*, *69*, 71–77.

Butin, H. (1975) Beitrag zur ascomyceten flora von Chile. *Sydowia*, 27, 267–292.

Butin, H. (1986) *Rhizothyrium paraskicum* sp. nov. (Coelomycetes), ein blattparasit auf *Araucaria araucana* (Mol.) C. *Koch*. *Journal of Phytopathology*, 115, 313–317.

Butin, H. & Peredo, H.L. (1986) Hongos parásitos en coníferas de América del Sur, con especial referencia a Chile. *Bibliotheca Mycologica*, 101, 1–100.

CONAF. (2018) Consejo de la Sociedad Civil CONAF se interioriza de daño que afecta a araucarias. Available at: https://www.conaf.cl/consejo-de-la-sociedad-civil-conaf-se-interioriza-de-dano-que-afecta-a-araucarias/ [Accessed 1 February 2021]

Crous, P., Schumacher, R.K., Akulov, A., Thangavel, R., Hernández-Restrepo, M., Carnegie, A. et al. (2019) New and interesting fungi. 2. *Fungal Systematics and Evolution*, 3, 57–134.

Crous, P., Wingfield, M., Guarro, J., Cheewangkoon, R., van der Bank, M., Swart, W. et al. (2016) Fungal Planet description sheets: 469–557. *Persoonia*, 37, 218.

Diaz, H.F., Grosjean, M. & Graumlich, L. (2003) Climate variability and change in high elevation regions: past, present and future. *Climatic Change*, 59, 1–4.

Duong, T.A., De Beer, Z.W., Wingfield, B.D. & Wingfield, M.J. (2013) Characterization of the mating-type genes in *Leptographium procerum* and *Leptographium profanum*. *Fungal Biology*, 117, 411–421.

Fitzpatrick, H.M. (1920) Monograph of the Coryneliaceae. *Mycologia*, 12, 206–237.

Fitzpatrick, H.M. (1942a) Revisionary studies in the Coryneliaceae. *Mycologia*, 34, 464–488.

Fitzpatrick, H.M. (1942b) Revisionary studies in the Coryneliaceae. II. The genus *Caliciopsis*. *Mycologia*, 34, 489–514.

Funk, A. (1963) Studies in the genus *Caliciopsis*. *Canadian Journal of Botany*, 41, 503–543.

Garreaud, R.D., Boisier, J.P., Rondanelli, R., Montecinos, A., Sepúlveda, H.H. & Veloso-Aguila, D. (2020) The central Chile mega drought (2010–2018): a climate dynamics perspective. *International Journal of Climatology*, 40, 421–439.

Garrido-Benavent, I. & Pérez-Ortega, S. (2015) Unravelling the diversity of European *Caliciopsis* (Coryneliaceae, Ascomycota): *Caliciopsis valentina* sp. nov. and *C. beckhausii* comb. nov., with a worldwide key to *Caliciopsis*. *Mycological Progress*, 14, 10.

González, G. & Opazo, A. (2002) Enfermedades fungosas y otras. In: Baldini, A. and Pancel, L. (Eds.) *Agentes de Daño en el Bosque Nativo*. Santiago de Chile: Editorial Universitaria, pp. 89–199.

González, M.E. & Veblen, T.T. (2006) Climatic influences on fire in *Araucaria araucana–Nothofagus* forests in the Andean cordillera of south-central Chile. *Écoscience*, 13, 342–350.

Guerrero, N.R., Quintero, M.A.O. & Naranjo, J.C.P. (2012) Determinación del área foliar en fotografías tomadas con una cámara web, un teléfono celular o una cámara semiprofesional. *Revista Facultad Nacional de Agronomía – Medellín*, 65, 6399–6405.

Herrmann, T.M. (2005) Knowledge, values, uses and management of the *Araucaria araucana* forest by the indigenous Mapuche Pewenche people: a basis for collaborative natural resource management in southern Chile. *Natural Resources Forum*, 29, 120–134.

Kalyaanamoorthy, S., Minh, B.Q., Wong, T.K., von Haeseler, A. & Jermiin, L.S. (2017) ModelFinder: fast model selection for accurate phylogenetic estimates. *Nature Methods*, 14, 587.

Katoh, K., Rozewicki, J. & Yamada, K.D. (2019) MAFFT online service: multiple sequence alignment, interactive sequence choice and visualization. *Briefings in Bioinformatics*, 20, 1160–1166.

Kershaw, P. & Wagstaff, B. (2001) The southern conifer family Araucariaceae: history, status, and value for paleoenvironmental reconstruction. *Annual Review of Ecology and Systematics*, 32, 397–414.

Kumar, S., Stecher, G. & Tamura, K. (2016) MEGA7: molecular evolutionary genetics analysis version 7.0 for bigger datasets. *Molecular Biology and Evolution*, 33, 1870–1874.

Léveillé, J. (1846) Descriptions des champignons de l'herbier du Muséum de Paris. *Annales des Sciences Naturelles (Ser.*, 3) 5, 249–305.

McCormack, H.W. (1936) The morphology and development of *Caliciopsis pinea*. *Mycologia*, 28, 188–196.

Mellado-Mansilla, D., Díaz, I.A., Godoy-Güinao, J., Ortega-Solís, G. & Moreno-Gonzalez, R. (2018) Bosque Pehuén Park's flora: a contribution to the knowledge of the Andean montane forests in the Araucanía Region, Chile. *Natural Areas Journal*, 38, 298–311.

Migliorini, D., Luchi, N., Pepori, A.L., Pecori, F., Aglietti, C., Maccioni, F. et al. (2020) *Caliciopsis moriondi*, a new species for a fungus long confused with the pine pathogen *C. pinea*. *MycoKeys*, 73, 87–108.

Munck, I.A., Livingston, W., Lombard, K., Luther, T., Ostrofsky, W.D., Weimer, J. et al. (2015) Extent and severity of caliciopsis canker in New England, USA: An emerging disease of eastern white pine (*Pinus strobus* L.). *Forests*, 6, 4360–4373.

Pascoe, I., Smith, I., Dinh, S.-Q. & Edwards, J. (2018) *Caliciopsis pleomorpha* sp. nov. (Ascomycota: Coryneliales) causing a severe canker disease of *Eucalyptus cladocalyx* and other eucalypt species in Australia. *Fungal Systematics and Evolution*, 2, 45–56.

Pérez, S., Guerrero, J. & Galdames, R. (2018) First report of *Neofusicoccum nonquaesitum* in Chile causing branch dieback and decline in *Araucaria araucana*. *Plant Disease*, 102, 1460.

Pratibha, J., Amandeep, K., Shenoy, B. & Bhat, D. (2010) *Caliciopsis indica* sp. nov. from India. *Mycosphere*, 1, 65–72.

Ramsfield, T., Bentz, B., Faccoli, M., Jactel, H. & Brockerhoff, E. (2016) Forest health in a changing world: effects of globalization and climate change on forest insect and pathogen impacts. *Forestry*, 89, 245–252.

Rayner, R.W. (1970) *A Mycological Colour Chart*. Kew, UK: Commonwealth Mycological Institute and British Mycological Society.

Rehner, S.A. & Samuels, G.J. (1995) Molecular systematics of the Hypocreales: a teleomorph gene phylogeny and the status of their anamorphs. *Canadian Journal of Botany*, 73, 816–823.

Rodriguez, R., Matthei, S. & Quezada, M.M. (1983) *Flora Arbórea de Chile*. Concepción: Editorial de la Universidad de Concepción.

Schumacher, V., Justino, F., Fernández, A., Meseguer-Ruiz, O., Sarricolea, P., Comin, A. et al. (2020) Comparison between observations and gridded data sets over complex terrain in the Chilean Andes: Precipitation and temperature. *International Journal of Climatology*, 40, 5266–5288.

Simler-Williamson, A.B., Rizzo, D.M. & Cobb, R.C. (2019) Interacting effects of global change on forest pest and pathogen dynamics. *Annual Review of Ecology, Evolution, and Systematics*, 50, 381–403.

Trifinopoulos, J., Nguyen, L.-T., von Haeseler, A. & Minh, B.Q. (2016) W-IQ-TREE: a fast online phylogenetic tool for maximum likelihood analysis. *Nucleic Acids Research*, 44, W232–W235.

Vélez, M.L., Marfetán, J.A., Salgado Salomón, M.E. & Taccari, L.E. (2020) *Mortierella* species from declining *Araucaria araucana* trees in Patagonia, Argentina. *Forest Pathology*, 50, e12591.

Vélez, M.L., Salgado Salomón, M.E., Marfetan, A., Tirante, S.I., Mattes, F.H., Avila, M. et al. (2018) *Caracterización Desecación del Dosel y Sanidad de* Araucaria araucana *en Argentina*. Technical report. Available at: https://doi.org/10.13140/RG.2.2.14227.78889 [Accessed 6 August 2020]

Vilgalys, R. & Hester, M. (1990) Rapid genetic identification and mapping of enzymatically amplified ribosomal DNA from several *Cryptococcus* species. *Journal of Bacteriology*, 172, 4238–4246.

Wang, F. (2017) SIOX plugin in ImageJ: area measurement made easy. *UV4Plants Bulletin*, 2016, 37–44.

White, T.J., Bruns, T., Lee, S. & Taylor, J. (1990) Amplification and direct sequencing of fungal ribosomal RNA genes for phylogenetics. In: Innis, M.A., Gelfand, D.H., Sninsky, J.J. and White, T.J. (Eds.) *PCR Protocols: A Guide to Methods and Applications*. New York: Academic Press, pp. 315–322.

Zapata, M. & Schafer, M. (2019) *Diplodia africana* causing twig death on *Araucaria araucana*, a new host and first record for Chile. *New Disease Reports*, 40, 2.

How to cite this article: Balocchi FA, Wingfield MJ, Ahumada R, Barnes I. *Pewenomyces kutranfy* gen. nov. et sp. nov. causal agent of an important canker disease on *araucaria araucana* in chile. *Plant Pathol*. 2021;00:1–17. https://doi.org/10.1111/ppa.13353

SUPPORTING INFORMATION

Additional supporting information may be found online in the Supporting Information section.